

Performance Improvement of UWB-sensor Positioning using Multiple Filters

Seong-Hyeon Choi¹ and Jae-Hong Yim^{2,+}

Abstract

This study highlights the increasing research on transportation-robot technology in the logistics industry, smart farms, and smart factories with the advancement of Internet of Things technology. The current state of real-time location-tracking systems in transportation-robot systems is analyzed, existing issues are identified, and experiments are conducted to enhance system performance. While traditional location-tracking technologies are expensive and complex, the ultra-wideband (UWB)-sensor precision-improvement method proposed in this study aims to achieve high-precision positioning data at a low cost by combining multiple filters. The experiments in this study are conducted using an integrated interface device for data processing that was designed and manufactured considering the actual environment. Real-time positioning data are obtained by applying various filters, including the Kalman, Median, and Min filters, to a real-time positioning system using UWB sensors. The acquired data are analyzed by comparing the results before and after applying the filters for three types of errors: mean error, maximum error, and the number of data points exceeding a 5-cm error range. The results of this study are expected to be applicable to various location-based fields, such as logistics and automation robots, in the future.

Keywords: UWB sensor, Kalman filter, Median filter, Min filter, AMR

1. INTRODUCTION

In recent years, technological advances in transport robots have significantly accelerated in the fields of robotics, logistics, smart farming, and smart-factory industries with the rapid growth of Internet of Things applications. The domestic logistics-robot market has experienced a compound annual growth rate (CAGR) of 13.8% from 2017 to 2022, accompanied by numerous efforts to advance artificial intelligence-based robotics applications [1]. The overall annual growth rate is projected to reach an average of 40% by 2025. In smart farms and factories, transport robots are expected to perform a range of tasks, such as crop harvesting and material handling, where the precise processing of sensor and motor data is crucial. Currently, the core technologies that drive autonomous robots include control systems utilizing various sensors, such as

light detection and ranging, three-dimensional depth cameras, and simultaneous localization and mapping algorithms.

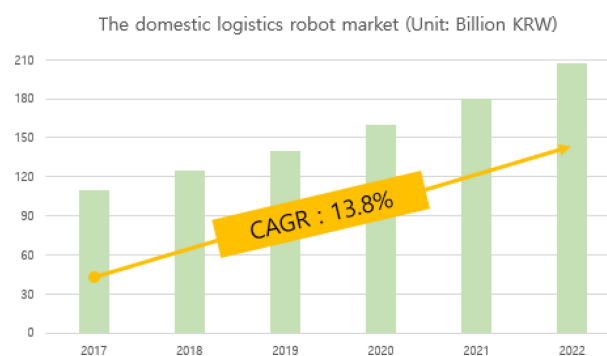


Fig. 1. CAGR of domestic logistics-robot market

These control systems must evolve into high-performance robots equipped with interfaces capable of processing diverse sensor data in real-time to meet the precision and stability demands of logistics transport and service tasks, even if these systems require high development and production costs. However, the implementation of high-performance robotics remains a challenge for simple repetitive-motion tasks and control systems; thus, individuals cannot easily adopt them in real-life scenarios or simple platform-based systems. The accuracy of sensor data is crucial when operating sensor-based robots. While high-

¹Graduate School of Korea Maritime & Ocean University
727 Taejong-ro, Yeongdo-Gu, Busan 49112, Korea

²Department of Electronics & Communications Engineering, Korea Maritime & Ocean University
727 Taejong-ro, Yeongdo-Gu, Busan 49112, Korea

⁺Corresponding author: jhyim@kmou.ac.kr

(Received: Nov. 6, 2024, Revised: Nov. 11, 2024, Accepted: Jan. 6, 2025)

This is an Open Access article distributed under the terms of the Creative Commons Attribution Non-Commercial License(<https://creativecommons.org/licenses/by-nc/3.0/>) which permits unrestricted non-commercial use, distribution, and reproduction in any medium, provided the original work is properly cited.

performance sensors enable accurate data processing, they also increase production costs. Conversely, low-performance sensors may produce inaccurate data, leading to suboptimal performance and increased data-processing frequency.

Currently, positioning technologies employing ultra-wideband (UWB) sensors enable real-time indoor tracking and the development of various location-based platforms. Numerous research studies have focused on enhancing positioning accuracy by integrating Kalman filters and GPS-based solutions [2,3].

In this study, we apply Kalman filters as well as the Median and Min filters in seven combinations to improve the precision of UWB-sensor positioning data. These combinations include the (1) Kalman filter, (2) Median filter, (3) Min filter, (4) Median and Kalman filters, (5) Min and Kalman filters, (6) Min and Kalman filters, and (7) a combination of the Median, Min, and Kalman filters. This approach aims to compare positioning data with and without filters to identify the optimum filtering algorithms with enhanced performance. Subsequently, a drive platform based on a brushless direct-current (BLDC) motor is developed, and the driving performance is evaluated after implementing the optimal filter algorithms.

2. EXPERIMENTAL

This section describes the experimental setup used to verify the precision improvement of the UWB sensors as well as the integrated interface device and driving platform used for the filter application and data acquisition. High-performance automated guided vehicles typically achieve a positioning accuracy of less than 1 cm, whereas autonomous mobile robots (AMRs) achieve a positioning accuracy of less than 3–5 cm. Given that the baseline accuracy of the DWM1001 sensor is within 10 cm, this experiment aims to achieve a positioning accuracy of less than 5 cm, which meets the requirements of high-performance robots.

Additionally, during the operation of the driving platform equipped with a UWB sensor, a single anchor is placed at the designated destination, allowing the platform to navigate there by processing real-time distance data between the left and right tags [4,5,6]. Based on the processed positioning data, the revolutions per minute (RPM) of the left and right BLDC motors are controlled to compare and analyze the straight-line driving performance with and without the application of sensor filters [7,8,9].

2.1 Measurement setup



Fig. 2. 1-m fixed profile

To ensure a uniform height and distance during the experiment, we prepared three 1-m profiles, as shown in Fig. 2. Two tags (left and right) and one anchor were used to verify the positioning data between the tag and anchor, and each positioning data point was recorded at intervals of 200 ms.

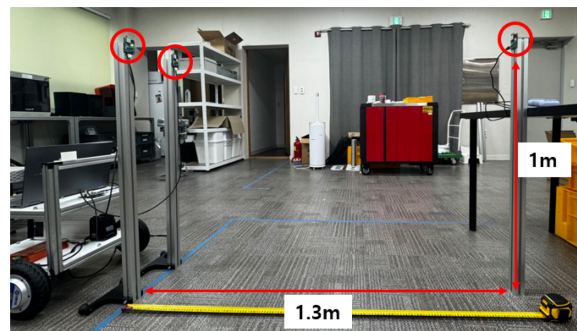


Fig. 3. UWB position-measurement setup

The left and right tags and anchor sensor were positioned at a fixed height of 1 m and fixed distance of approximately 1.3 m (Fig. 3). Approximately 300 data samples were acquired under various filter combinations at the fixed distance, and the precision of the distance between each tag and the anchor was analyzed. The initial positions of the left and right tags were not aligned in order to acquire data based on raw measurements without positional correction. Instead, data analysis was performed using the initial positions at which they were installed.

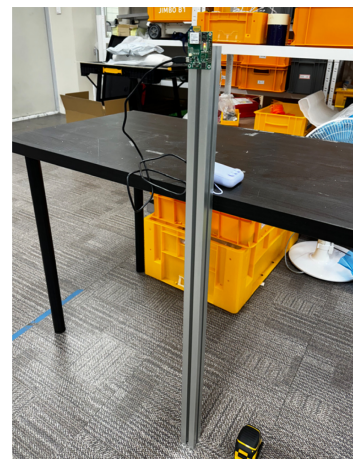


Fig. 4. Fixed anchor



Fig. 5. Two fixed tags (left and right)

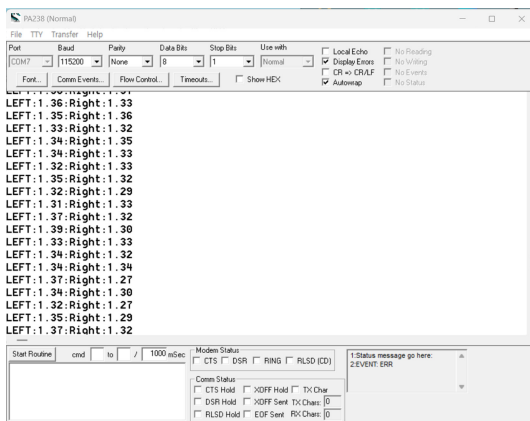


Fig. 6. Positioning-data format

As shown in Fig. 4, a single anchor was fixed at the destination, and two tags (left and right) were fixed as shown in Fig. 5. The positioning data from the anchor were compared and analyzed for each tag to estimate data reliability. To compare the driving performance of the platform with and without the filter application, the distance between the two tags was fixed to match the left and right distances of the driving platform.

The positioning data were obtained via HyperTerminal, converted into the CSV format, and represented as graphs for comparative analysis (Fig. 6). The positioning-data format used “,” as a delimiter, with measurements obtained in meters with two decimal places based on a reference of 1.3 m.

2.2 Integrated interface device

The integrated interface is a hardware device used for processing positioning data with multiple filters and driving BLDC motors. It comprises a communication-interface board between the UWB sensor and BLDC motor driver, modules for tags and anchors, and the driving platform.

2.2.1 Integrated interface board

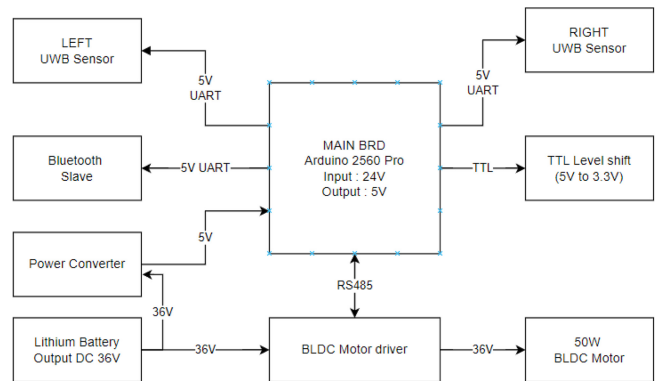


Fig. 7. Configuration diagram of the integrated interface board

The communication-interface board controls the positioning data of the two tags (left and right) and BLDC motor driver (Fig. 7). A 36 V lithium-ion battery was connected in series to the BLDC motor driver to supply power, and the voltage was converted from 36 V to 5 V to power the Bluetooth signal, tags (left and right), and Arduino 2560 Pro. The communication-interface board processes the positioning data received from the UWB sensors in real time via universal asynchronous receiver/transmitter (UART) communication and controls the 50 W BLDC in-wheel motor through the motor driver using RS485 communication based on the Modbus RTU protocol.

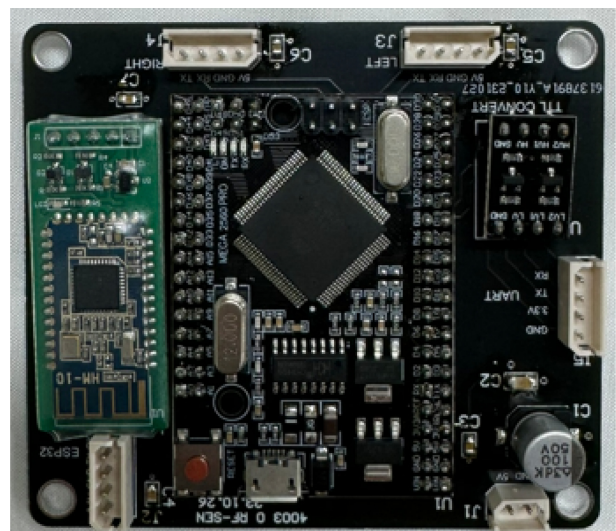


Fig. 8. Integrated interface board

The PCB layout in Fig. 8 shows the completed board, which was designed with two tag UART ports on the top, an RS485 on the lower left side, and power ports on the lower right side.

2.2.2. Anchor module

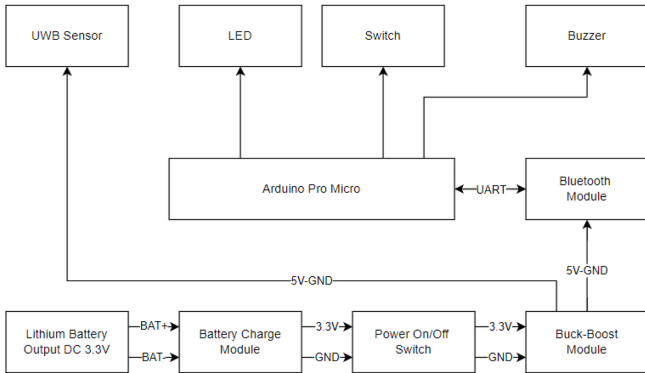


Fig. 9. Configuration of anchor module

The anchor module remotely controls the operation of the integrated interface device and the start and end of the data acquisition from the UWB sensor. The anchor module was powered by a lithium-ion battery with an additional charging module (Fig. 9). A buck-boost circuit was adopted to step up the power supply from 3.7 V to 5 V for the Arduino Pro micro, Bluetooth module, and other devices. The design includes an LED for status indication, a control switch, and a buzzer, and utilizes wireless communication via the Bluetooth module for interaction with the integrated interface device [10].

2.2.3 Tag module



Fig. 11. Tag-module PCB

The tag module was designed to ensure a seamless connection with the communication interface board via UART communication by supplying the operating voltage to the DWM1001. As shown in Fig. 11, the DWM1001 module was mounted and connected to the communication interface board via a four-pin connector at the bottom [10].

2.2.4 Driving platform

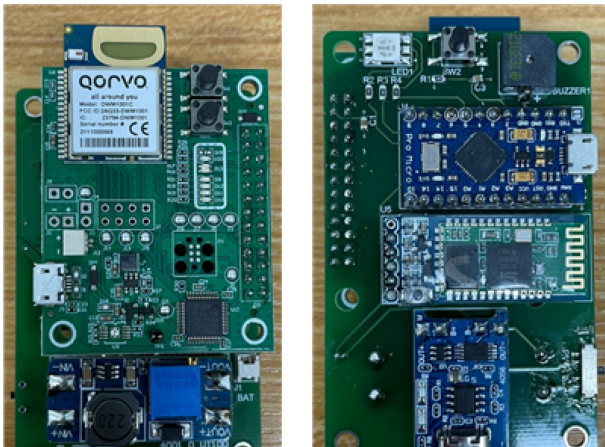


Fig. 10. Anchor-module PCB

As illustrated in Fig. 10, the PCB was fabricated based on the circuit layout and was assembled with the UWB sensor and components on both sides. The DWM1001 module was installed on the front side of the PCB, whereas the interface components, Arduino Pro Micro, Bluetooth, and battery-charge module were installed on the back side.



Fig. 12. Driving platform

The driving platform was developed to obtain straight-line driving-performance data based on UWB sensor-positioning data. A comparative analysis was conducted between the driving performance without filter application and that with the optimized filter. As shown in Fig. 12, the platform was equipped with two tag modules (left and right) and two BLDC motors (left and right) mounted at the top. In addition, the 36 V lithium-ion battery, BLDC motor driver, and communication-interface board were installed inside. A laptop was mounted on top of the module to acquire the positioning data in real time.

3. RESULTS AND DISCUSSIONS

3.1 Positioning-data comparison

3.1.1 Normal positioning data

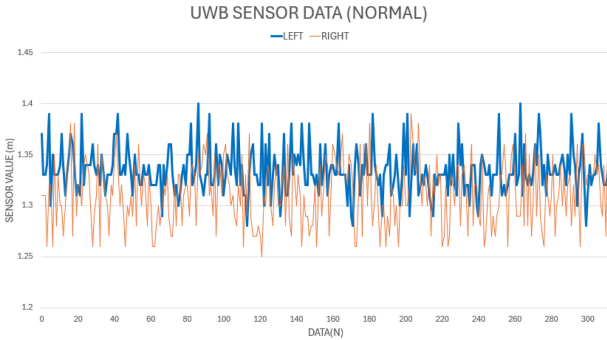


Fig. 13. Normal positioning data (blue line: left tag; orange line: right tag)

Table 1. Comparison of normal positioning-data accuracy for left and right tags

Tag	Mean error (cm)	Maximum error (cm)	Instances exceeding 5 cm
Left	1.45	8	21
Right	1.19	9	27

3.1.2 Positioning data with the Kalman filter

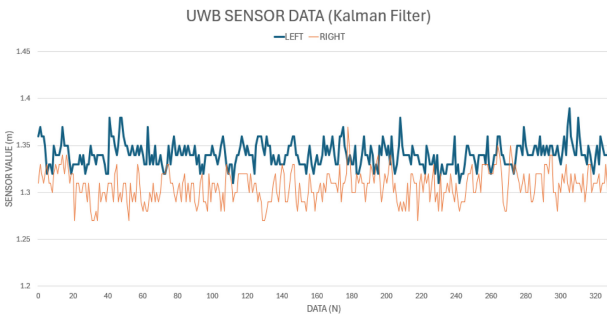


Fig. 14. Positioning data after applying the Kalman filter (blue line: left tag; orange line: right tag)

Table 2. Comparison of positioning accuracy for left and right tags after applying the Kalman filter

Tag	Mean error (cm)	Maximum error (cm)	Instances exceeding 5 cm
Left	1.06	6	1
Right	1.71	7	1

3.1.3 Positioning data with Median filter

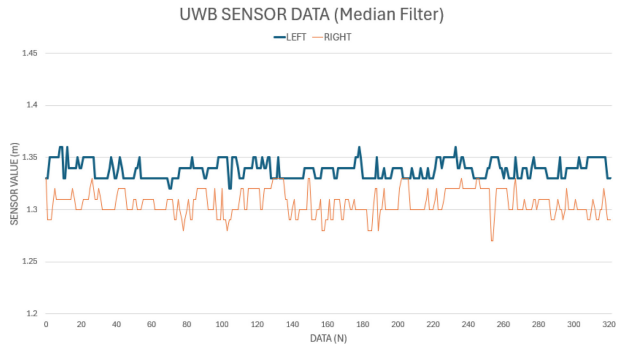


Fig. 15. Positioning data after applying the Median filter (blue line: left tag; orange line: right tag)

Table 3. Comparison of positioning accuracy for left and right tags after applying the Median filter

Tag	Mean error (cm)	Maximum error (cm)	Instances exceeding 5 cm
Left	0.81	3	0
Right	0.64	3	0

3.1.4 Positioning data with Min filter

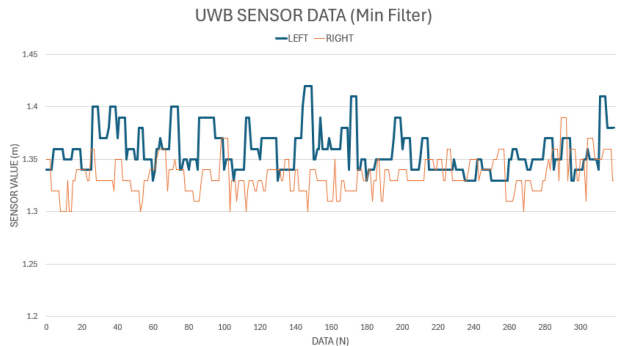


Fig. 16. Positioning data after applying the Min filter (blue line: left tag; orange line: right tag)

Table 4. Comparison of positioning accuracy for left and right tags after applying the Min filter

Tag	Mean error (cm)	Maximum error (cm)	Instances exceeding 5 cm
Left	2.90	9	44
Right	3.52	9	32

3.1.5 Positioning data with Median and Kalman filters

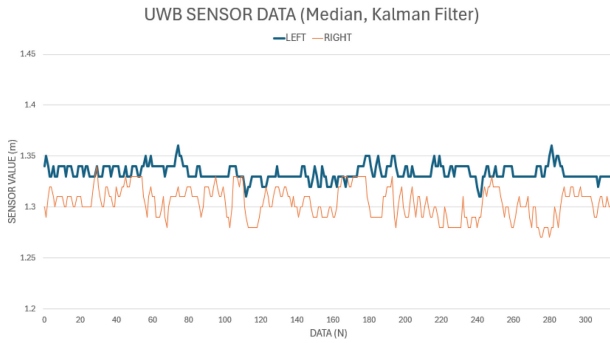


Fig. 17. Positioning data after applying the Median and Kalman filters (blue line: left tag; orange line: right tag)

Table 5. Comparison of positioning accuracy for left and right tags after applying the Median and Kalman filters

Tag	Mean error (cm)	Maximum error (cm)	Instances exceeding 5 cm
Left	0.39	3	0
Right	0.44	4	0

3.1.6 Positioning data with Min and Kalman filters

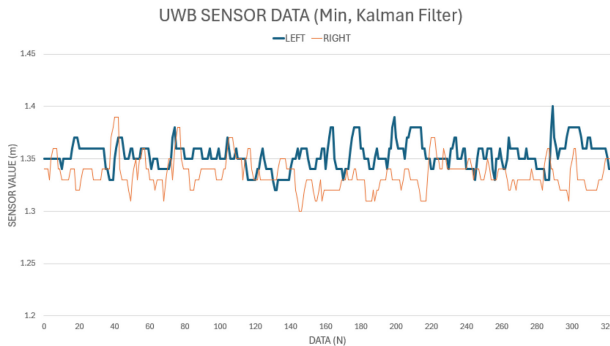


Fig. 18. Positioning data after applying the Min and Kalman filters (blue line: left tag; orange line: right tag)

Table 6. Comparison of positioning accuracy for left and right tags after applying the Min and Kalman filters

Tag	Mean error (cm)	Maximum error (cm)	Instances exceeding 5 cm
Left	3.34	8	19
Right	3.55	9	28

3.1.7 Positioning data with Median and Min filters

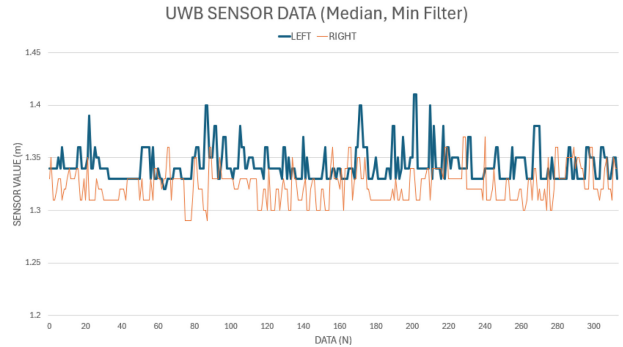


Fig. 19. Positioning data after applying the Median and Min filters (blue line: left tag; orange line: right tag)

Table 7. Comparison of positioning accuracy for left and right tags after applying the Median and Min filters

Tag	Mean error (cm)	Maximum error (cm)	Instances exceeding 5 cm
Left	1.30	8	8
Right	2.40	7	16

3.1.8 Positioning data with Median, Min, and Kalman filters

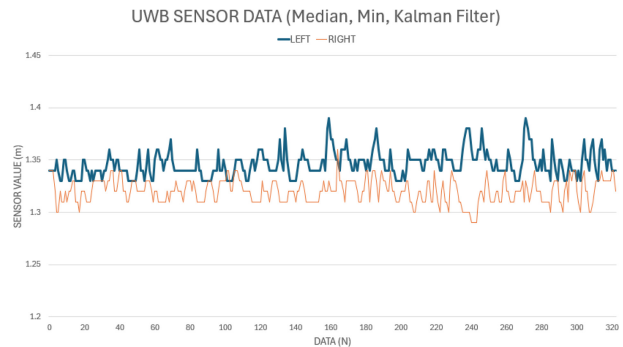


Fig. 20. Positioning data after applying the Median, Min, and Kalman filters (blue line: left tag; orange line: right tag)

Table 8. Comparison of positioning accuracy for left and right tags after applying Median, Min, and Kalman filters

Tag	Mean error (cm)	Maximum error (cm)	Instances exceeding 5 cm
Left	1.30	8	8
Right	2.40	7	16

3.1.9 Normal driving-platform performance

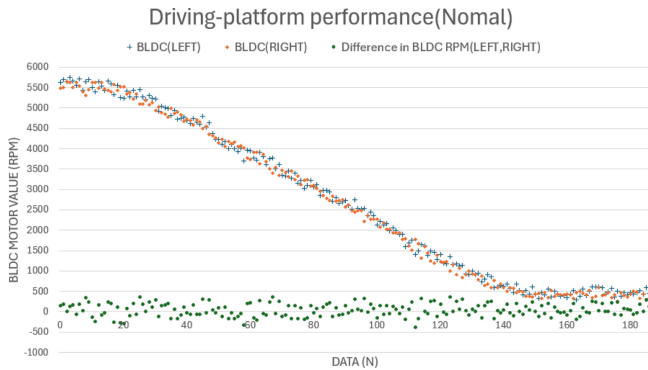


Fig. 21. Normal driving-platform performance

Fig. 21 shows the driving-performance graph of the platform using unfiltered positioning data. Owing to the errors in the positioning data, the left and right BLDC motors operated independently at irregular RPMs until they reached their destination (anchor). Consequently, the RPM difference between the left and right BLDC motors fluctuated by approximately 500 RPM, resulting in an unstable driving performance.

3.1.10 Driving-platform performance with Median and Kalman filters

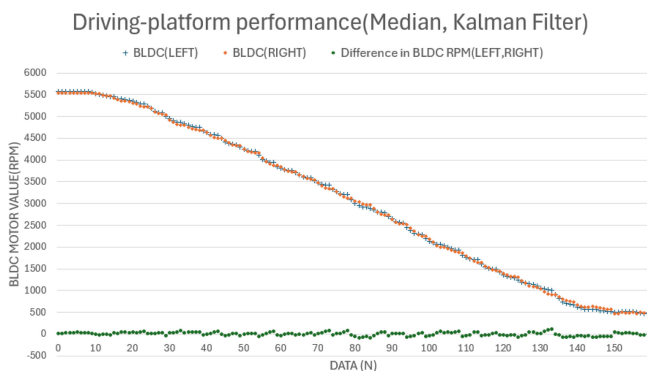


Fig. 22. Driving-platform performance after applying the Median and Kalman filters

Fig. 22 shows a performance graph of the driving platform using the positioning data processed with the Median and Kalman filters proposed in this study [11]. Until the destination (anchor) was reached, the left and right BLDC motors were driven individually at a regular RPM owing to the enhanced accuracy of the positioning data. Consequently, the difference in the BLDC RPM (left and right) approached 0 RPM, demonstrating smooth driving performance.

4. CONCLUSIONS

The real-time positioning system tracks the relative positions of the tag and anchor by sharing positioning data based on triangulation. This system is advantageous for obtaining precise position data both indoors and outdoors by minimizing the interference from other wireless communications. The positioning system aims to improve the accuracy of cost-effective UWB-positioning data and integrate it into a driving platform to enhance driving performance.

To improve the accuracy of the UWB sensor, we combined the Kalman, Median, and Min filters, compared their performances, and suggested an optimal filter combination. The tag and anchor modules were designed using a DWM1001 UWB sensor, and a communication-interface board and driving platform were designed and manufactured to process the positioning data in real time.

Experiments were conducted at a fixed distance of approximately 1.3 m and at the same height of 1 m using combinations of the Kalman, Median, and Min filters to acquire positioning data. We compared and analyzed the maximum error, average error, and number of data points with precision exceeding 5 cm. The positioning data without filter application exhibited a maximum error of 8–9 cm, a number of data points exceeding 5-cm precision ranging from 21 to 27, and an average error of 1.20–1.45 cm based on approximately 300 data points. In contrast, the combination of the Median and Kalman filters demonstrated a maximum error of 3–4 cm, with 0 data points exceeding 5-cm precision, and an average error of 0.39–0.44 cm based on the same number of data points. These data indicate improvements in the average error by 63%–73% and maximum error by 56%–63%, as well as a 100% reduction in data exceeding 5-cm precision, thereby demonstrating the enhanced precision of the positioning data of the UWB sensor.

The Min filter output the smallest value from the positioning data, which typically led to the processing of the values with the largest errors from the normal data. Consequently, applying the Min filter led to a significant increase in the average error, maximum error, and number of data points exceeding 5-cm precision compared with the normal data, resulting in the decreased precision of the UWB sensor.

Among the seven filter combinations, the combination of the Median and Kalman filters demonstrated the most significant performance improvement. When applied to the driving platform, the smoothest driving performance was exhibited when traveling

directly to the destination from a distance of 5 m. The resulting positioning accuracy was considered similar to that of high-performance AMRs (with a positioning accuracy of less than 3–5 cm). The utilization of low-cost UWB sensors is expected to facilitate their application in simple repetitive movements and position-based systems. In the future, we plan to research solutions for potential precision-deterioration factors that may arise when processing multiple anchor- and tag-based systems simultaneously. We also intend to explore methods for improving precision by applying moving averages over time.

REFERENCES

- [1] <https://www.lotis.or.kr/news/4407> (retrieved on Jul. 07, 2024).
- [2] H. Kim, “Enhanced UWB Positioning System Using Kalman Filter”, M. S. Thesis, Graduate School of Kwangwoon University, Seoul, 2017.
- [3] J. Lee, “Improving Indoor Positioning Accuracy Using GNSS and UWB”, M. S. Thesis, Graduate School of Sungkyunkwan University, Seoul, 2023.
- [4] Federal Communications Commission (FCC), Revision of Part 15 of the Commission’s Rules Regarding Ultra-Wideband Transmission Systems, Federal Communications Commission (FCC), Washington, 2002.
- [5] K. Siwiak and D. McKeown, *Ultra-Wideband Radio Technology*, Hoboken, Wiley, NJ, pp. 1-241, 2004.
- [6] ISO/IEC, Information Theory - Real Time Location System (RTLS), International Standard ISO/IEC 24730-2, 2006.
- [7] T. H. Kim and M. Ehsani, “Sensorless control of the BLDC motors from near-zero to high speeds”, *IEEE Trans. Power Electron.*, Vol. 19, No. 6, pp. 1635-1645, 2004.
- [8] T. J. E. Miller, “Brushless permanent-magnet motor drives”, *Power Eng. J.*, Vol. 2, No. 1, pp. 55-60, 1998.
- [9] J. Kim, “A Study on the Design of a High-Performance Sensorless BLDC Motor Drive IC Using ADC”, M. S. Thesis, Graduate School of University of Seoul, Seoul, 2013.
- [10] <https://www.qorvo.com/products/p/DWM1001C#documents> (retrieved on Jul. 07, 2024).
- [11] S. Jeong and D. Choi, “Development of a Real-Time Position Tracking System for a Manufacturing Process Based on a UWB Sensor Using a Kalman Filter”, *J. Kor. Acad.-Ind. Cooperation Soc.*, Vol. 21, No. 1, pp. 627-633, 2020.